Quantitative picosecond laser-induced fluorescence measurements of nitric oxide in flames

Brackmann, Christian; Bood, Joakim; Nauclér, Jenny D.; Konnov, Alexander A.; Aldén, Marcus

Published in:
Proceedings of the Combustion Institute

DOI:
10.1016/j.proci.2016.07.012

2017

Document Version:
Publisher's PDF, also known as Version of record

Available online at www.sciencedirect.com

ScienceDirect

Proceedings of the Combustion Institute 36 (2017) 4541–4548

Proceedings of the Combustion Institute

www.elsevier.com/locate/proci

Quantitative picosecond laser-induced fluorescence measurements of nitric oxide in flames

Christian Brackmann*, Joakim Bood, Jenny D. Nauclér, Alexander A. Konnov, Marcus Aldén

Division of Combustion Physics, Department of Physics, Faculty of Engineering, Lund University, P.O. Box 118, SE-221 00 Lund, Sweden

Received 3 December 2015; accepted 5 July 2016
Available online 18 July 2016

Abstract

Quantitative concentrations measurements using time-resolved laser-induced fluorescence have been demonstrated for nitric oxide (NO) in flame. Fluorescence lifetimes measured using a picosecond Nd:YAG laser and optical parametric amplifier system have been used to directly compensate the measured signal for collisional quenching and evaluate NO concentration. The full evaluation also includes the spectral overlap between the ~15 cm^{-1} broad laser pulse and multiple NO absorption lines as well as the populations of the probed energy levels. Effective fluorescence lifetimes of 1.2 and 1.5 ns were measured in prepared $NO/N_2/O_2$ mixtures at ambient pressure and temperature and in a premixed NH_3-seeded $CH_4/N_2/O_2$ flame, respectively. Concentrations evaluated from measurements in $NO/N_2/O_2$ mixtures with NO concentrations of 100–600 ppm were in agreement with set values within 3% at higher concentrations. An accuracy of 13% was estimated by analysis of experimental uncertainties. An NO profile measured in the flame showed concentrations of ~1000 ppm in the post-flame region and is in good agreement with NO concentrations predicted by a chemical mechanism for NH_3 combustion. An accuracy of 16% was estimated for the flame measurements. The direct concentration evaluation from time-resolved fluorescence allows for quantitative measurements in flames where the composition of major species and their collisional quenching on the probed species is unknown. In particular, this is valid for non-stationary turbulent combustion and implementation of the presented approach for measurements under such conditions is discussed.

Keywords: Laser-induced fluorescence; Nitric oxide; NO; Concentration measurements

1. Introduction

Laser-induced fluorescence (LIF) is a widely used technique for species detection in combustion diagnostics. The method is attractive due to its high sensitivity, high spatial and temporal resolution, imaging capacity, and high species-specificity

* Corresponding author.
E-mail address: christian.brackmann@forbrf.lth.se (C. Brackmann).

http://dx.doi.org/10.1016/j.proci.2016.07.012

in many measurement situations. Comprehensive reviews of LIF for combustion studies can be found in [1–3] and an overview focusing on imaging applications is given in Aldén et al. [4]. While the list of qualitative studies using LIF is extensive and for example contains advanced applications such as monitoring locations of certain chemical reactions or dynamic behavior of specific quantum states, combustion studies with quantitative species concentrations measured with LIF are fewer.

Even though the fluorescence signal carries information about the concentration of the probed species, quantitative measurements are challenging, as they require knowledge about multiple parameters that influence the relation between the measured signal and the absolute species concentration. In combustion, the natural lifetime of excited states of chemical species is normally much longer than typical molecular collision times (~100 ps for an atmospheric-pressure flame), thus the vast majority of the population in the excited state is removed by other processes than spontaneous emission, i.e. fluorescence. The fluorescence quantum yield, i.e. the ratio between the number of spontaneously emitted and absorbed photons, is often the parameter most difficult to assess as it is affected by collision processes, stimulated emission, predissociation, and photoionization. While the latter three effects can be circumvented – stimulated emission and photoionization by low-intensity excitation and predissociation by avoiding excitation to predissociative states – the impact of collisional processes is more problematic to deal with since they are dependent on temperature, pressure, chemical composition, and the quantum states involved. In addition, collisional processes influence absorption lineshapes and hence the spectral overlap between the absorption line and the laser profile.

It is possible to account for these effects through measurements in calibration flames or by measuring the composition of major species and temperature, from which collisional quenching rates can be determined. While the former approach mainly works for stationary flames, the latter is in principle also applicable for turbulent flames, given that all quenching species and the temperature can be measured simultaneously and that quenching cross sections for all species are available. Such simultaneous measurements may require an excessive and complex experimental system, although combined single-pulse Raman/Rayleigh/LIF measurements have been demonstrated [5]. Moreover, comprehensive data sets of quenching cross sections are only available for a few diatomic species, and incomplete or even nonexistent for more complex species.

There are a number of experimental approaches for which the influence of collisions on the fluorescence signal is reduced, such as saturated LIF [6], predissociative LIF [7,8], and photo-ionization controlled loss spectroscopy [9]. In practice it is, however, not possible to obtain completely collision-free detection with these methods. The spatial, spectral, and temporal shapes of laser pulses are generally non-uniform and need to be considered as complete saturation is not achieved across the entire laser pulse. These issues have however been thoroughly investigated, see e.g. Lucht et al. and references therein [6], and when accounted for properly, saturated LIF enables quantitative species concentration measurements of for example OH [6,10,11] and NO [12–14]. For predissociative LIF and photo-ionization controlled loss spectroscopy, fluorescence yields are typically very low resulting in low sensitivity. Moreover, the methods are often limited to low pressures, typically up to 1 atm, as the quenching rate increases with pressure and eventually becomes comparable with the predissociation/photoionization rate.

The collisional quenching rate, and hence the fluorescence quantum yield, can be directly determined by measuring the fluorescence signal temporally resolved, which requires laser pulses significantly shorter than the fluorescence lifetime. Typical fluorescence lifetimes in combustion environments are in the range 1–10 ns and excitation using picosecond laser pulses together with a fast detector, such as a streak camera or a fast photomultiplier tube, is normally required. Quenching rate determination based on fluorescence lifetime measurements has been made in various atmospheric-pressure flames for a number of combustion species, such as O [15], NO [16], OH [17,18], CH [19], CO [20], and CH_2O [21].

While fluorescence lifetimes allow extraction of fluorescence quantum yields, a number of additional parameters, i.e. the aforementioned spectral overlap of the laser pulse and absorption spectrum, the fractional population in the probed energy level/levels, the fluorescence collection efficiency, and the detector responsivity, must also be determined in order to retrieve absolute species concentrations from LIF measurements. Execution of all these steps in the same experiment, directly yields absolute concentrations and this paper describes the complete procedure for such quantitative measurements. The approach is demonstrated and characterized for measurements of nitric oxide (NO) concentrations in gas mixtures at ambient pressure and temperature as well as in a premixed laminar NH_3-seeded $CH_4/N_2/O_2$ flame. In addition, the feasibility of the procedure for single-shot measurements, required for studies in turbulent combustion environments, is discussed.

2. Methods

2.1. Experimental

The 355 nm third harmonic radiation generated by a mode-locked picosecond Nd:YAG laser (Ekspla, PL 2143C) with external amplifier (Ekspla, APL 70-1100), pumps an OPG/OPA unit (Ekspla PG401-P80-SH) providing tunable radiation in the

ultraviolet regime. The laser produces pulses of 80 ps duration at a repetition rate of 10 Hz. While the laser provides pulse energies of ~0.4 mJ at wavelengths around 226 nm, typically 20 μJ was employed for excitation of NO. The laser beam was directed towards the flame using a Pellin–Broca prism and a half-wave plate together with a polarizer cube were employed to control the laser pulse energy and to ensure a vertically polarized beam. The beam was focused into a small horizontal sheet, ~5 mm wide, using a cylindrical lens of focal length 300 mm. Fluorescence was collected at right angle relative to the laser beam and imaged onto the horizontal entrance slit of a streak camera (Optronis, OptoScope, 19.5 × 14.4 mm CCD chip with 1392 × 1024 pixels) using a spherical lens of focal length 100 mm. The streak camera enables time-resolved measurements and produces images where the horizontal and vertical axis represents time and position along the slit, respectively. Fluorescence decay curves for data evaluation were obtained by averaging over pixels along the direction of the streak camera slit corresponding to spatial positions over a distance of 18 mm parallel to the burner. A spectrometer of focal length 75 cm (Andor, SR-750-A-R), having gratings of 300/2400 grooves/mm, and coupled to an intensified CCD camera (Andor, iStar) was employed for detection of an NO fluorescence emission spectrum and to monitor wavelength and spectral profile of the picosecond laser pulses.

Calibration measurements were made at ambient pressure and temperature on a prepared mixture of 2 molar percent NO in N_2 (accuracy ±2%) which was further diluted with air to achieve mixtures of different NO concentration in the range 100-600 ppm. Measurements were also made in a flat one-dimensional flame stabilized on a water-cooled stainless steel porous-plug burner (Holthuis & Associates). Methane, oxygen, nitrogen, and ammonia (AGA Gas AB, purity 99.9%) were supplied to the burner via mass-flow controllers (Bronkhorst) at flow rates of 0.7, 1.4, 8.4, and 0.056 l/min, respectively. This resulted in a stoichiometric flame with reactants CH_4:NH_3:O_2:N_2 in proportions 0.066:0.0052:0.13:0.80. A steel plug was mounted 1.6 cm above the burner surface to enhance flame stabilization. The burner and stabilizer were mounted on a stage allowing for accurate translation of the flame relative to the laser beam and detector. Flame temperature profiles were measured using a type R thermocouple ($d = 0.5$ mm) to be used for evaluation of LIF data as well as input for flame modeling carried out using CHEMKIN-PRO and the stagnation plane module [22]. Simulations included multicomponent diffusion transport, thermal diffusion, and were made with a grid of ~800 points obtained with the parameters GRAD = 0.5 and CURV = 0.02. Simulations were made with a fixed temperature profile obtained by spline interpolation of experimental temperatures. A detailed kinetic mechanism of 97 species and 779 reactions, developed for ammonia-doped methane combustion at oxy-fuel conditions by Mendiara and Glarborg [23], was used for the modeling. The mechanism has been experimentally validated in a flow reactor for $CH_4/NH_3/O_2/N_2$ mixtures at atmospheric pressure and in the temperature range 973–1773 K [23].

The NO excitation wavelength, 226.05 nm, was chosen as the wavelength resulting in the strongest signal obtained while scanning the laser wavelength across the NO (0-0) band. Measurements were made using a streak rate of 500 ps/mm and a 0.5 mm slit width on the streak camera. In addition to NO fluorescence, Rayleigh scattering measurements were made in nitrogen at ambient conditions to calibrate the signal collection efficiency and to monitor the temporal response function of the detector. Time-resolved Rayleigh scattering signals indicate a temporal resolution of 280 ps, determined from the full-width at half the maximum of the signal. For each measurement point, at different heights above the burner in the flame and for different NO concentrations in the calibration measurements, data were averaged over 100 pulses. Backgrounds were acquired with the laser tuned to ~227 nm i.e. a spectral position off the NO (0-0) band. Pulse energies were monitored for each measurement point using a power meter (Gentec, SOLO 2).

2.2. Data evaluation

According to the discussion on fluorescence presented in Eckbreth [1] the population of the excited final state, N_f (index f = final), decays after the laser pulse according to Eq. (1).

$$N_f = N_i^0 \tau_{laser} b_{if} \cdot e^{-\frac{t}{\tau_{eff}}} \tag{1}$$

In Eq. (1) N_i^0 represents the initial population of the probed initial state (index i = initial), τ_{laser} is the laser pulse duration and b_{if} the rate coefficient for absorption transitions between states i and f. The product of these quantities, $N_i^0 \tau_{laser} b_{if}$, represents the population of the excited state established during the duration of the laser pulse. The fluorescence signal is proportional to N_f and can be expressed according to Eq. (2).

$$S_F(t) = h\nu \frac{\Omega}{4\pi} \varepsilon l A N_i^0 b_{if} A_{fi} \tau_{laser} \cdot e^{-\frac{t}{\tau_{eff}}} \tag{2}$$

In Eq. (2) h is Planck's constant, ν represents the fluorescence wavenumber, Ω the solid angle for detection, ε the detector efficiency, l the probe volume length, A the probe volume cross section area, A_{fi} the Einstein coefficient for spontaneous emission, and τ_{eff} the effective fluorescence lifetime. Following the discussion presented in Eckbreth [1] the absorption rate is related to the Einstein absorption

coefficient, B_{if}, according to Eq. (3)

$$b_{if} = \frac{B_{if}}{c} \int_{\nu} I_{\nu}(\nu) g(\nu) d\nu \tag{3}$$

where I_ν is the laser spectral irradiance expressed in unit $W\cdot(cm^2)^{-1}\cdot(cm^{-1})^{-1}$, c is the speed of light, and $g(\nu)$ represents an area-normalized profile of the NO absorption line. Expressing the laser spectral irradiance using a lineshape profile $L(\nu)$ normalized according to $\int_\nu L(\nu)d\nu = \Delta\nu$, where $\Delta\nu$ represents the laser spectral linewidth (full width at half maximum, FWHM), the absorption rate can be expressed according to Eq. (4)

$$b_{if} = \frac{B_{if} E}{\Delta\nu c \tau_{laser} A} \int_{\nu} L(\nu) g(\nu) d\nu \tag{4}$$

where E is the laser pulse energy. Inserting this into Eq. (2) results in the following expression for the fluorescence signal.

$$S_F(t) = h\nu \frac{\Omega}{4\pi} \varepsilon l N_i^0 \cdot \frac{B_{if} E}{\Delta\nu c} \int_{\nu} L(\nu) g(\nu) d\nu \cdot A_{fi} \cdot e^{-\frac{t}{\tau_{eff}}} \tag{5}$$

The factors related to the detection system can be retrieved by calibration versus Rayleigh scattering for which the signal integrated over a laser pulse can be expressed according to Eq. (6)

$$S_{Rayleigh} = E_{Rayleigh} N_{ref} \Omega \varepsilon l \left(\frac{\partial\sigma}{\partial\Omega}\right) \tag{6}$$

where $E_{Rayleigh}$ is the laser pulse energy during Rayleigh scattering measurements, N_{ref} is the total gas number density in the probe volume, and $(\frac{\partial\sigma}{\partial\Omega})$ is the differential Rayleigh scattering cross section. Integration of the fluorescence signal $S_F(t)$ over time yields

$$\int_0^{t_f} S_F(t) dt = h\nu \frac{\Omega}{4\pi} \varepsilon l N_i^0 \cdot \frac{B_{if} E}{\Delta\nu c} \int_{\nu} L(\nu) g(\nu) d\nu \cdot A_{fi} \cdot \tau_{eff} (1 - e^{-\frac{t_f}{\tau_{eff}}}) \tag{7}$$

Equation (7) can be solved for N_i^0 and the total NO number density is obtained by introducing the Boltzmann factor f_i, representing the population fraction of level i. Combined with Eq. (6) this results in

$$N_{NO} = \frac{4\pi \Delta\nu c \int_0^{t_f} S_F(t) dt \cdot E_{Rayleigh} N_{ref} \left(\frac{\partial\sigma}{\partial\Omega}\right)}{f_i h\nu A_{fi} S_{Rayleigh} E B_{if} \tau_{eff} (1 - e^{-\frac{t_f}{\tau_{eff}}}) \int_{\nu} L(\nu) g(\nu) d\nu} \tag{8}$$

Equation (8) is valid for excitation of a single transition and emission in a single fluorescence band. However, the rather broad spectral profile of the picosecond laser pulse covers multiple NO rotational transitions and the fluorescence is emitted in multiple vibrational bands. To include these properties Eq. (8) needs to be modified with summations over multiple excitation lines, j, and multiple emission bands, k, according to Eq. (9).

$$N_{NO} = \frac{4\pi \Delta\nu c \int_0^{t_f} S_F(t) dt \cdot E_{Rayleigh} N_{ref} \left(\frac{\partial\sigma}{\partial\Omega}\right)}{h E S_{Rayleigh} \tau_{eff} (1 - e^{-\frac{t_f}{\tau_{eff}}}) \sum_k \left(\nu_k A_{fi,k}\right) \cdot \sum_j \left(f_{i,j} B_{if,j} \int_{\nu} L(\nu) g_j(\nu) d\nu\right)} \tag{9}$$

The evaluation procedure is outlined in the flow chart shown in Fig. 1. Experimental temperatures and NO spectral line positions retrieved from LIFBASE [24] are used for calculation of line broadening. Lineshapes $g_j(\nu)$ were calculated as Voigt profiles with Lorenzian and Gaussian components determined from collisional and Doppler broadening, respectively. Collisional broadening was calculated using parameters for NO reported by Chang et al. [25] thus taking the effects of pressure on the absorption lineshape into account in the evaluation. The laser lineshape $L(\nu)$ was determined experimentally and fitted by a Voigt profile centered at 44,234 cm^{-1} with FWHM 14.9 cm^{-1}. The spectrally broad profile of the OPG/OPA result in a time-bandwidth product of 36, and compared with the value of 0.44 for a transform-limited Gaussian profile it is clear that the pulses are far from transform-limited. The spectral profile is illustrated in Fig. 2 together with part of the NO absorption spectrum at 1400 K, corresponding to conditions prevailing in the post-flame region of the investigated flame.

The main NO transitions covered by the laser are P_1(21-23), P_2(27-28), Q_1(11-14), Q_2(20-21), R_1(5-8), and R_2(14-15), all of which needs to be considered in terms of absorption coefficient, line overlap integral, and population factor when evaluating the signal. Using the laser spectral profile together with lineshapes and Einstein coefficients for absorption, $B_{if,j}$, for each transition, allowed for calculation of absorption rates as shown in Eq. (4). Rotational population factors $f_{i,j}$ for the experimental temperature were also retrieved from LIFBASE and these quantities combined allowed for calculation of the summation over index j in Eq. (9).

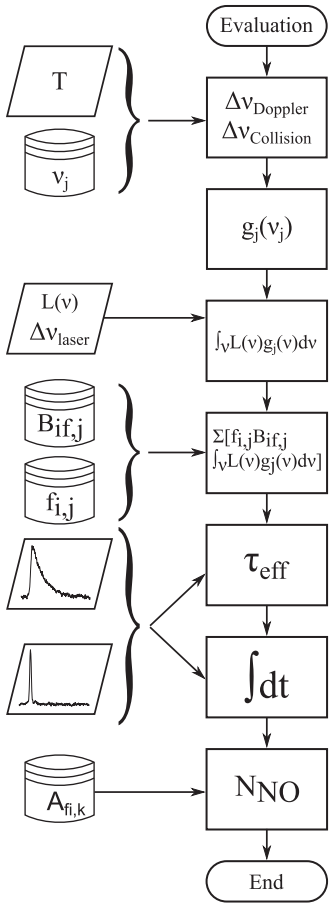

Fig. 1. Flow chart of the evaluation procedure for time-resolved fluorescence data. Input data from experiments and database (LIFBASE) are shown in the left column with trapezoid and cylinder symbols, respectively while calculation steps are shown in the right column. Temperature and NO spectral line positions are used for calculation of line broadening and lineshapes g_j. The laser spectral profile L allows for calculations of overlap integrals, which are combined with Einstein absorption coefficients $B_{if,j}$ and populations fractions $f_{i,j}$. Effective fluorescence lifetimes, τ, are evaluated from experimental fluorescence decay curves and a Rayleigh scattering signal. Time integrals of these signals are further used in the calculations which also include Einstein coefficients for spontaneous emission, $A_{fi,k}$.

The effective fluorescence lifetime τ_{eff} for NO in $NO/N_2/O_2$ mixtures was determined by fitting a single exponential function, convoluted with the instrument function determined from Rayleigh scattering measurements, to experimental fluorescence decay curves. In the flame, chemical composition, temperature and fluorescence lifetimes can be expected to be constant in the post-flame region. However, due to spread in lifetimes evaluated for data measured in adjacent points in the post-flame

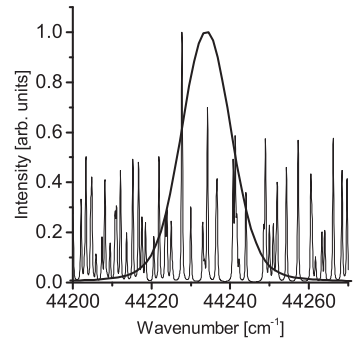

Fig. 2. Voigt profile FWHM = 14.9 cm^{-1} representing the picosecond laser spectral lineshape together with rotational lines of the NO (0-0) band. The laser overlaps with multiple transitions in the P-,Q-, and R-branches.

region and consequently in the evaluated concentration profiles, an alternative evaluation approach was investigated. Using this method, the lifetime was determined from the time integral of a peak-normalized fluorescence decay curve, which resulted in less spread of the values obtained in the post-flame region and a more uniform NO concentration profile. The integration likely suppresses some noise and therefore this method was employed for evaluation of flame data.

The Rayleigh signal was integrated over the time interval covered by the streak camera including the entire laser pulse whereas the fluorescence decay signal was integrated from the time where the integrated Rayleigh signal had reached 90% of its maximum value. The Rayleigh scattering cross section was determined from data presented by Miles et al. [26]. Wavenumbers, ν_k, and Einstein coefficients for spontaneous emission, $A_{fi,k}$, for NO fluorescence emission bands were also obtained from LIFBASE and used for calculation of the summation over index k in Eq. (9).

3. Results and discussion

Figure 3 shows NO fluorescence decay curves measured in a mixture of $NO/N_2/O_2$, and in the post-flame zone of the premixed NH_3-seeded $CH_4/N_2/O_2$ flame. The corresponding fluorescence lifetimes are 1.2 and 1.5 ns, respectively. Lifetime calculations for the mixture using reported NO quenching cross sections for collisions with N_2 and O_2 compiled by Drake and Ratcliffe [27] give values in the range 1.09–1.54 ns. The fluorescence lifetime of 1.2 ns is in good agreement with a lifetime of 1.09 ns obtained using cross sections measured by Drake and Ratcliffe for fluorescence in the (2-0) band [27]. Nevertheless, it should be noted that our value is based on the emission from multiple NO bands. The major components of the flame product gas are N_2, H_2O, and CO_2 in approximate percent-

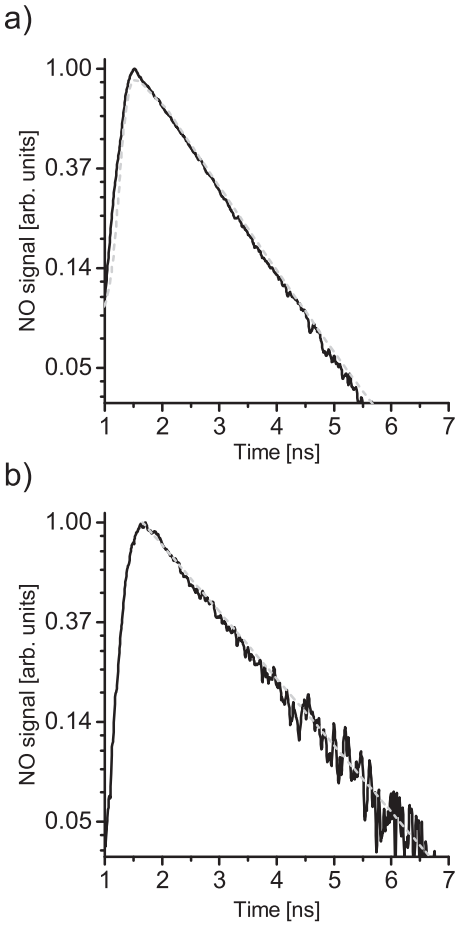

Fig. 3. Experimental NO fluorescence decay curves (solid lines). (a) Measured in $NO/N_2/O_2$ mixture at ambient conditions, effective fluorescence lifetime 1.2 ns. (b) Measured in a premixed NH_3-seeded $CH_4/N_2/O_2$ flame, effective fluorescence lifetime 1.5 ns. Fitted single-exponential decay curves are shown as dashed gray profiles.

ages of 80%, 14% and 6%, respectively. Calculation using quenching cross sections presented by Drake and Ratcliffe [27] and Tamura et al. [28], assuming a temperature of 1300 K, results in effective lifetimes of 1.44 and 1.54 ns, respectively. The effective lifetimes evaluated for the flame product zone are in the range 1.4 to 1.8 ns and thus show good agreement with results reported in literature.

Figure 4 shows NO concentrations evaluated for measurements on $NO/N_2/O_2$ mixtures of known compositions. The straight line represents values where the evaluated and experimental concentrations would be equal. The uncertainty of the NO concentration level in the prepared NO/N_2 mixture was stated to be 2%, which combined with the accuracy of the massflow controllers and their calibration device result in a total uncertainty of 3% for the investigated $NO/N_2/O_2$ mixtures. The

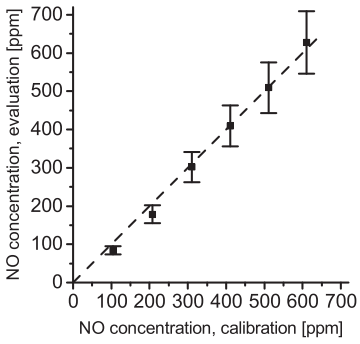

Fig. 4. Evaluated NO concentrations from time-resolved fluorescence measurements versus concentrations of $NO/N_2/O_2$ mixtures. The error bars represent a 13% uncertainty estimated for the experimental data. The dashed line represents points were experimental and evaluated concentrations would be equal.

error bars in Fig. 4 indicate the estimated uncertainty in the NO concentrations evaluated from LIF data. Repeated measurements indicate uncertainties of 5% in laser pulse energy for measurements of NO fluorescence as well as Rayleigh scattering. The inaccuracy of the laser wavenumber was estimated to be on the same order as the instrumental broadening of the spectrograph, i.e. 2.6 cm^{-1}. Evaluations shifting the laser wavenumber by this value resulted in changes in evaluated NO concentrations by 6%. The impact of the laser FWHM was assessed by evaluation using a laser spectral profile determined without considering the instrument response function of the spectrometer, i.e. a laser linewidth 1.2 cm^{-1} broader, which changed the evaluated concentrations by 4%. Diagnostic methods based on absolute signal strengths require careful background subtraction and a test of the sensitivity to variations in background was made by evaluation using two equivalent but separately measured backgrounds, which resulted in NO concentrations differing by 3%.

An analysis of the lifetime evaluation routine was carried out by checking the impact of including the laser pulse in the evaluation. Neither evaluation of the decay over a time interval after the laser pulse nor excluding convolution with the laser pulse altogether resulted in any changes in the evaluated lifetime. The quality of the fits suggests that any uncertainties introduced by the lifetime evaluation procedure can be considered negligible compared with the other sources of uncertainty outlined above. In addition to laser pulse energy, the accuracy of the detection system calibration is also dependent on Rayleigh cross section and differences in detector response between the laser wavelength and the wavelengths of the NO fluorescence bands. The Rayleigh cross section uncertainty depends on the accuracy of the measured laser wavelength and is expected to be less

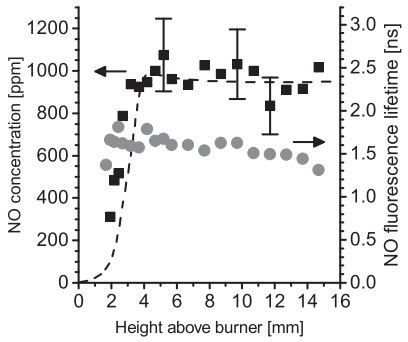

Fig. 5. NO profiles of premixed laminar flat $CH_4/N_2/O_2$ flame seeded with 5000 ppm NH_3. Experimental data (square symbols) are shown together with a prediction (dashed line) from a mechanism by Mendiara and Glarborg [23]. The error bars represent a 16% uncertainty estimated for the experimental data. The effective fluorescence lifetimes evaluated from the fluorescence decay curves are shown in grey circles.

than 1%. The streak camera response varies by approximately 7% over the wavelength interval of the strong NO bands. Considering factors estimated to be less than 1% negligible and all uncertainties to be independent the total uncertainty, calculated as the root-sum-square, is determined to be 13% represented by the error bars on the data points in Fig. 4. Nevertheless, directly using the measured quantities in the evaluation results in very good agreement with differences less than 3% between evaluated and experimental NO concentrations for values of 300 ppm and higher. The two lowest evaluated NO concentrations are under-predicted by 19 and 14%, respectively, even though the error bars are fairly close to the dashed line. At low concentrations and NO signals accurate background subtraction becomes more critical, however investigations of experimental data showed no indications of background subtraction errors and background analysis as mentioned above merely changed the evaluated concentration by a few ppm. Skalska et al. have reported on oxidation of NO into NO_2 at ambient conditions [29] and this process would reduce NO concentrations in the prepared $NO/N_2/O_2$ mixtures. However, the time for transport from the point of mixing to the measurement position is on the order of a second or less, and for the reaction rates reported [29] no appreciable decrease in NO concentration would be observed. However, ineffective mixing and some gas retention effects at the lowest flows might in combination with some amount of NO oxidation be a possible explanation for the underestimation.

Figure 5 shows NO concentration profiles, measured in the NH_3-seeded $CH_4/N_2/O_2$ flame and obtained from simulation using the mechanism of Mendiara and Glarborg [23], and the evaluated effective lifetimes, discussed previously. In the post-flame region at height 4 mm above the burner and higher, where a homogenous NO distribution is expected, the average experimental NO concentration is 972 ppm while the corresponding value from the model is 964 ppm. Thus, experimental data show very good agreement with model prediction and a difference of less than 1%. Nevertheless, data show some scatter and flame measurements introduce a temperature uncertainty, in addition to the uncertainties identified for the NO mixtures. Thermocouple measurements show a maximum flame temperature close to 1390 K, with an estimated accuracy of ±70 K. Data evaluation with temperature profiles shifted ±70 K resulted in changes in evaluated number densities of 4%, thus representing the combined temperature sensitivity of the temperature-dependent factors in the evaluation. Moreover, calculations of relative concentrations also include the temperature resulting in additional temperature-dependent uncertainty. The corresponding changes in evaluated NO concentrations were 10%, to be included with the 13% assigned to the measurements of the mixtures. Altogether, this results in an overall uncertainty of 16% for the flame measurements represented by the error bars inserted in Fig. 5. Some improvement in accuracy could be achieved using Coherent anti-Stokes Raman Spectroscopy (CARS) thermometry, which has an accuracy of ∼50 K at flame temperatures.

The results of Fig. 5 clearly show that a time-resolved fluorescence signal measured in flame can be directly evaluated to retrieve quantitative species concentrations. This is a distinct advantage since the composition of major species and their collisional quenching on the probed species is often unknown in flames. In particular, this is valid for non-stationary conditions requiring single-shot measurements. Data acquired in the post-flame region above 4 mm where NO concentrations are around 970 ppm show a signal-to-noise ratio (SNR) of ∼11 and a detection limit of 250 ppm corresponding to an SNR of 3 can be estimated. Assuming shot-noise-limited detection, single-shot measurements would decrease the SNR by a factor of 10 resulting in a detection limit increased by the same factor. However, the laser system allows for pulse energies in the range 400–500 μJ, which would increase the signal as excitation is carried out in the linear regime. In addition, the detection sensitivity could be enhanced by one order of magnitude using a micro-channel photomultiplier tube. These improvements combined would increase the single-shot signal by a factor of ∼200 and improve the single-shot SNR by a factor of 14 resulting in a detection limit of ∼180 ppm, similar to that of the averaged data. Further rearrangements, such as focusing the laser beam into a single point and carefully optimized signal collection might provide additional improvement of the single-shot detection limit. In studies of turbulent combustion,

imaging measurements are desirable and can be achieved using fluorescence lifetime imaging [30]. Combing fluorescence lifetime imaging with the presented evaluation approach would in principle allow for quantitative imaging measurements under non-stationary conditions. However, simultaneous temperature measurements as well as knowledge on the single-shot variations of the laser spectral profile are necessary for evaluation and to assess measurement accuracy.

4. Conclusion

Direct quantitative concentration measurements based on time-resolved fluorescence has been demonstrated for NO in flame. The approach does not rely on any calibration for determination of molecular parameters or separate measurements of quenching rates but permits quenching correction and concentration evaluation directly from time-resolved data acquired in flame. Concentrations evaluated from measurements on prepared gas mixtures at ambient pressure and temperature showed good agreement with experimental values. At concentration levels above 300 ppm data showed agreement within 3% with experimental values while individual uncertainties in experimental parameters were estimated to add up to a total uncertainty of 13%. Measurement in a premixed laminar NH_3-seeded flame showed very good agreement with predictions by a chemical mechanism for NH_3 combustion. For the flame an increased total uncertainty of 16% was estimated due to additional uncertainty in temperature. The approach allows for quantitative measurements in flames where the composition of major species and their collisional quenching on the probed species is unknown. In particular, this is valid for non-stationary turbulent combustion for which the presented approach could be applicable for single-point measurements using sensitive fast detectors.

Acknowledgments

The authors gratefully acknowledge financial support from the Swedish Research Council, the Centre for Combustion Science and Technology (CECOST), the Knut and Alice Wallenberg foundation, and the European Research Council through Advanced Grant TUCLA (669466).

References

[1] A.C. Eckbreth, *Laser Diagnostics for Combustion Temperature and Species*, Gordon and Breach, Amsterdam, Netherlands, 1996.
[2] K. Kohse- Höinghaus, *Prog. Energ. Combust.* 20 (1994) 203–279.
[3] K. Kohse-Höinghaus, J.B. Jeffries, *Applied Combustion Diagnostics*, Taylor&Francis, New York, 2002.
[4] M. Aldén, J. Bood, Z.S. Li, M. Richter, *Proc. Combust. Inst.* 33 (2011) 69–97.
[5] F. Fuest, R.S. Barlow, J.Y. Chen, A. Dreizler, *Combust. Flame* 159 (2012) 2533–2562.
[6] R.P. Lucht, D.W. Sweeney, N.M. Laurendeau, *Combust. Flame* 50 (1983) 189–205.
[7] P. Andresen, A. Bath, W. Groger, H.W. Lulf, G. Meijer, J.J. Termeulen, *Appl. Opt.* 27 (1988) 365–378.
[8] T.S. Cheng, J.A. Wehrmeyer, R.W. Pitz, O. Jarrett, G.B. Northam, *Combust. Flame* 99 (1994) 157–173.
[9] J.T. Salmon, N.M. Laurendeau, *Opt. Lett.* 11 (1986) 419–421.
[10] M.C. Drake, R.W. Pitz, M. Lapp, et al., *Twentieth Symposium (International) on Combustion* 20 (1985) 327–335.
[11] R.P. Lucht, D.W. Sweeney, N.M. Laurendeau, M.C. Drake, M. Lapp, R.W. Pitz, *Opt. Lett.* 9 (1984) 90–92.
[12] R.V. Ravikrishna, C.S. Cooper, N.M. Laurendeau, *Combust. Flame* 117 (1999) 810–820.
[13] B. Li, Y. He, Z.S. Li, A.A. Konnov, *Combust. Flame* 160 (2013) 40–46.
[14] Z.H. Wang, Y.J. Zhou, R. Whiddon, Y. He, K.F. Cen, Z.S. Li, *Combust. Flame* 164 (2016) 283–293.
[15] F. Ossler, J. Larsson, M. Aldén, *Chem. Phys. Lett.* 250 (1996) 287–292.
[16] R. Schwarzwald, P. Monkhouse, J. Wolfrum, *Chem. Phys. Lett.* 158 (1989) 60–64.
[17] M. Kollner, P. Monkhouse, *Appl. Phys. B-Lasers O* 61 (1995) 499–503.
[18] M. Kollner, P. Monkhouse, J. Wolfrum, *Chem. Phys. Lett.* 168 (1990) 355–360.
[19] M.W. Renfro, A. Chaturvedy, N.M. Laurendeau, *Combust. Sci. Technol.* 169 (2001) 25–43.
[20] F. Di Teodoro, J.E. Rehm, R.L. Farrow, P.H. Paul, *J. Chem. Phys.* 113 (2000) 3046–3054.
[21] D.I. Shin, G. Peiter, T. Dreier, H.R. Volpp, J. Wolfrum, *Proc. Combust. Inst.* 28 (2000) 319–325.
[22] Reaction Design, CHEMKIN-PRO 15101, San Diego, (2010).
[23] T. Mendiara, P. Glarborg, *Combust. Flame* 156 (2009) 1937–1949.
[24] J. Luque, D.R. Crosley, SRI International Report MP 99-009, (1999).
[25] A.Y. Chang, M.D. Dirosa, R.K. Hanson, *J. Quant. Spectrosc. Ra.* 47 (1992) 375–390.
[26] R.B. Miles, W.R. Lempert, J.N. Forkey, *Meas. Sci. Technol.* 12 (2001) R33–R51.
[27] M.C. Drake, J.W. Ratcliffe, *J. Chem. Phys.* 98 (1993) 3850–3865.
[28] M. Tamura, P.A. Berg, J.E. Harrington, et al., *Combust. Flame* 114 (1998) 502–514.
[29] K. Skalska, J.S. Miller, S. Ledakowicz, *Chem. Pap.* 64 (2010) 269–272.
[30] A. Ehn, O. Johansson, J. Bood, A. Arvidsson, B. Li, M. Aldén, *Proc. Combust. Inst.* 33 (2011) 807–813.